Smith, D. J., & Shirahatti, A. (2015). The effects of long range residual stress, elastic follow-up and applied load on creep crack incubation and material toughness. *Journal of Strain Analysis for Engineering Design*, *50*(7), 455-469. https://doi.org/10.1177/0309324715595315

The effects of long range residual stress, elastic follow-up and applied load on creep crack incubation and material toughness

D. J. Smith and A.M. Shirahatti

Solid Mechanics Group, Department of Mechanical Engineering, University of Bristol, Bristol, United Kingdom BS8 1TR

Abstract

Creep crack incubation of Type 316H stainless steel at 550°C is explored in this paper. Fracture mechanics specimens, subjected to combinations of residual and applied loads and in the presence of elastic follow-up, are tested. The design of two new test rigs is described. The rigs introduce planned levels of elastic follow-up together with combined residual and applied loading conditions to the specimens. A series of high temperature elastic-plastic and elastic-plastic-creep experiments is undertaken to compare experimentally determined values of elastic follow-up with theoretical values. A further series of fracture mechanics tests is performed to measure creep crack incubation and material toughness for samples subjected to constant load and for tests under combined loading with elastic follow-up. It is demonstrated that for tests subjected to the same initial reference stresses longer incubation times are attained for elastic follow-up tests compared to constant load tests. Also, combined loading tests exhibit longer creep crack incubation times based on the same measured material toughness obtained from constant load tests. This suggests that not all the available strain energy provided by combined loading to a specimen at high temperature contributes to creep crack incubation.

Keywords : Creep crack incubation, elastic follow-up, residual stress, Type 316H stainless steel

1. Introduction

Residual stresses play an important role in the life assessment of structural components operating at high temperature. Such stresses arise from misfit strains produced usually during component manufacture and final fabrication. One example is the residual stress created during welding of thick section austenitic stainless steels for power plant applications [1, 2], leading to the formation of cracks whilst operating at high temperature. To ensure that accurate life assessments are made it is necessary to understand how residual stresses interact with applied service loads. One route is to assume that the total stress is the sum of the applied and residual stresses. This assumes that both stresses are treated as primary stresses (e.g. load controlled). An alternative approach [3] is to consider residual stress as a secondary stress (e.g. displacement controlled). When the component is operating at high temperature and creeping the residual stress relaxes. In practice, the interaction of the residual and applied stress depends on how the region of interest in a component, such as a stress concentration, behaves and interacts with the surrounding material. This is illustrated in Figure 1. For the component in load control (as if a primary stress) the material creeps at the same stress. In displacement control, (as if a secondary stress) creep leads to stress

relaxation. Now consider a two bar structure as shown in Figure 1 subjected to displacement control. There is the potential for elastic follow-up during creep [4], i.e. as the thinner bar creeps the larger bar unloads and controls the stress applied to the thinner bar. Elastic follow-up occurs when the stiffness of part a structure having parallel or series load paths is reduced. This reduction in stiffness is a result of non-linear deformation such as plasticity, creep and the initiation and growth of cracks [5, 6, and 7]. Importantly, the elastic follow-up results in additional strain accumulation than would be expected from pure stress relaxation as illustrated in Figure 1 but less than for primary stress alone. A definition of elastic follow-up is provided later.

Although Figure 1 illustrates structural behaviour for either applied displacements or loads, structures containing combinations of primary and secondary stresses behave similarly. The contribution of a residual stress to the primary stress at the stress concentration depends not only on the accommodation of the original misfit through permanent deformation but it is also governed by the elastic follow-up caused by the changes in relative stiffness in the structure. The effects of elastic follow-up and relaxation of residual stresses, as a result of localised plastic deformation and fracture, were explored in detail through a series of experiments by Smith and co-workers [6, 7] using a multiple bar system.

Situations that lead to creep crack incubation in steels operating at high temperature have been mostly examined for primary loading (i.e. samples are subjected to constant load alone), [8]. Here incubation refers to the onset of creep crack growth from an existing defect. Based on load controlled tests the times for existing cracks to grow a certain distance have been related to material toughness, K_{mat}. [9, 10]. This is equivalent to fracture toughness for elastic-plastic fracture. For high temperature fracture K_{mat} is a function of the material's elastic-plastic and creep properties. The material toughness is then used within a high temperature failure assessment diagram (HTFAD) to determine the loading conditions in a structure for the extension of cracks by creep [9]. The structure can be subjected to a combination of primary and secondary loads and it is assumed that K_{mat} is a material property independent of the loading conditions.

More recently [11 – 13], work has examined the effect of residual stress (secondary stresses) on creep crack incubation. This is done by creating residual stresses that are self-equilibrating within laboratory specimens rather than the specimen being part of structure where the residual stresses are balanced within the structure. Turski, O'Dowd and their co-workers [11, 12] subjected notched laboratory specimens to prior in-plane compression to create residual stresses within the specimen to study the development of creep damage leading to creep crack incubation. Hossain et al [13] utilised local out-of-plane compression to induce near crack tip residual stresses in laboratory specimens. Again the conditions for the formation of creep damage ahead of a crack, with the residual stresses acting as the driving force, were examined but these studies did not determine whether material toughness for secondary loading was the same as for load control.

In these earlier studies [11 - 13] residual stresses were concentrated in a small volume of material, with stresses, near to the notch or crack tip, being highly tensile and changing rapidly to compressive stresses several millimetres away from the crack tip. Residual stresses were measured over relatively small distances ahead of the notch or crack using neutron and X-ray diffraction

techniques. Since residual stresses relax during creep, the tests were interrupted at different times to measure the change in residual stress. However, the rate of residual stress relaxation is proportional to the elastic follow-up, [6] and this was neither measured nor determined in the earlier work [11 - 13]. Consequently it is not known the extent to which additional creep created during elastic follow-up contributed to damage accumulation or simply reduced the initial misfit leading to relaxation of residual stresses.

In contrast to these earlier studies the experimental approach by Smith and co-workers [6, 7] assumes that the laboratory specimen is within a structure and the residual stresses self-balance throughout the structure. This is the method adopted for this research. The main purpose of this research was to determine whether creep crack incubation times and material toughness are the same when a fracture mechanics sample is subjected to combined primary and secondary loads. Simple test rigs were manufactured to permit measurement of the residual and applied stresses directly and at any time in a test. Two test rigs were created to provide two levels of elastic follow-up. The rigs were designed to operate at high temperature and to permit creep crack incubation to occur in specimens containing pre-existing cracks.

The remainder of the paper describes, in section 2, the design of the test rigs, with section 3 explaining the subsequent experimental studies. Test results are presented and discussed in section 4. It is revealed that there is continuous residual stress relaxation in the test rigs and the specimens. Compared to constant load tests it is shown that creep crack incubation times increase with decreasing levels of elastic follow-up, and the measured material toughness is a function of the loading conditions.

2. Test rig design

2.1 Conceptual design

Two new test rigs were constructed each based on a classical three bar system [6, 7] illustrated in Figure 2. The rigs were developed to introduce long range residual stresses into a laboratory specimen through strain incompatibility in the system. This system has several key features convenient for its application to high temperature creep. The magnitude and the interaction of the residual stress with the applied loading are a function of the initial misfit displacement and the relative stiffness of the system components. The subsequent creep behaviour of the system, with and without the application of additional loading, is governed by (a) the degree to which the misfit is accommodated by plastic and creep strain in the laboratory specimen and (b) the elastic follow-up caused by changes in system stiffness. Importantly, all elements of the system can be monitored for the applied and residual forces and displacements throughout a test.

Figure 2 shows an idealisation of the three bar system consisting of two side bars ‘B’ and a middle bar combination of bar ‘A’ and a fracture mechanics specimen. Bars A and B deform elastically and have stiffness k_A and k_B respectively. The fracture mechanics specimen has an initial stiffness, k_S. An initial misfit, X, between the bars, created by joining the bars together, introduces residual forces (or fit-up stresses) into the system. With the arrangement shown in Figure 2 there is tension

in both bar A and the fracture specimen with balancing compression in bars B. Alternatively, the system can be arranged so that bar A and the fracture mechanics specimen are in compression with balancing tension in bars B. With the fracture specimen in either tension or compression the residual force in bar A and specimen does not self-equilibrate across the section of the fracture mechanics specimen (i.e. not in internal equilibrium), but is in equilibrium with the net forces in the outer bars. As will be shown later, the system is designed so that non-linear deformation (plasticity and creep) is confined only to a localised region in the fracture mechanics specimen. The overall system can also be subjected to an external (applied) load.

In earlier work, Smith et al [6] showed that when a multiple bar system is subjected to combined residual and applied stresses, the system exhibits elastic follow-up when the central section of the system exhibits non-linear deformation. This earlier work used a round bar in the centre of the system and the same concept applies to the fracture mechanics specimen in the system shown in Figure 2. It is assumed that only the fracture mechanics specimen undergoes non-linear deformation and all other components in the system remain elastic. For example, assuming that the fracture mechanics specimen behaves as an elastic-perfectly plastic material with a reference stress and strain response as shown in Figure 3, the elastic follow-up factor is defined by

$$Z = \frac{\varepsilon_f - \varepsilon_e}{\varepsilon_i - \varepsilon_f} \quad (1)$$

where ε_f is the final total reference strain the fracture mechanics specimen achieved at the maximum load, ε_e is the elastic reference strain provided by the final reference stress, σ_f and ε_i is the initial elastic reference strain that the specimen would achieve at the maximum load if it had not exhibited plastic deformation. The elastic follow-up caused by the changes in stiffness in the system leads to additional strain accumulation in the sample as illustrated in Figures 1 and 3.

The elastic follow-up factor, Z, is a number that lies between ∞ (load control) and 1 (displacement control) and its value depends on the stiffness of the bars in the system relative to the fracture mechanics specimen. This is provided that the bars in the system remain elastic. The ratio, β, of the stiffness of bar A to the specimen stiffness (i.e. the series elements of the system) is given by

$$\beta = \frac{k_A}{k_s} \quad (2)$$

For a connecting bar A with circular section and diameter, d_A the stiffness is

$$k_A = \frac{\pi d_A^2 E_A}{4 L_A} \quad (3)$$

where E_A is Young's modulus, d_A diameter and L_A length of inner bar A.

The fracture mechanics specimen is a C(T) specimen and its elastic stiffness under pin loading is given by [14],

$$k_s = B_n E_s \left(\frac{1-{a_0}/{W}}{1+{a_0}/{W}}\right)^2 \begin{pmatrix} 2.163 + 12.219\left({a_0}/{W}\right) - 20.065\left({a_0}/{W}\right)^2 \\ -0.9925\left({a_0}/{W}\right)^3 + 20.609\left({a_0}/{W}\right)^4 \\ -9.9314\left({a_0}/{W}\right)^5 \end{pmatrix}^{-1} \quad (4)$$

where, B_n is the net section thickness of specimen, E_s is Young's modulus, a_0 is the initial crack length, and W is the width of the specimen.

The effective stiffness k_{eff} of bar A and the specimen is determined from

$$\frac{1}{k_{eff}} = \frac{1}{k_S} + \frac{1}{k_A} \quad (5)$$

The ratio, α_{eff} of the stiffness of the outer bar, $2k_B$ to the inner system stiffness k_{eff} (i.e. the parallel elements of the system) is given by

$$\alpha_{eff} = \frac{2k_B}{k_{eff}} \quad (6)$$

and assuming that the outer bars have circular cross sections, k_B is given by

$$k_{\boldsymbol{B}} = \frac{\pi d_B^2 E_B}{4L_{\boldsymbol{B}}} \quad (7)$$

where E_B is Young's modulus, d_B diameter and L_B length of outer bar B.

Smith et al [6] show that an overall elastic follow-up factor Z caused by changes in stiffness in the system is described by

$$Z = Z_{eff} Z_S \quad (8)$$

where

$$Z_{eff} = \frac{1+\alpha_{eff}}{\alpha_{eff}} \text{ and } Z_S = \frac{1+\beta}{\beta} \quad (9)$$

A detailed derivation of this is given in [6]. Figure 3 shows the inverse of the overall elastic follow-up factor, Z as a function of the relative effective stiffness ratio, α_{eff} and the series stiffness ratio, β. Displacement controlled conditions correspond to a combination of high values of β and α_{eff} i.e. when the inverse of elastic follow-up factor tends to 1. However as β decreases the system tends towards more load controlled conditions i.e. as the inverse of the elastic follow-up

tends to zero. Between the extremes of load and displacement control there are mixed boundary conditions (i.e. neither displacement nor load controlled conditions) on the fracture mechanics specimen.

A residual stress state is created in the system by introducing an initial misfit, X, between the outer bars and the central bar and specimen. It can be shown that the residual force, F_S^R is given by [6, 7]

$$F_S^R = k_S X \frac{\alpha_{eff}}{1+\alpha_{eff}} \tag{10}$$

The residual force in the fracture specimen is a function of three parameters; the stiffness of the specimen, the initial misfit and the relative stiffness of the assembly. If any of these parameters change as a result of subsequent loading then on unloading the level of residual force will change. If the specimen undergoes sufficient permanent deformation equal to the initial misfit displacement the initial force reduces to zero. Further details of how changes to either the stiffness or misfit influence the magnitudes of the residual force are explored by Aird et al [7]. Equations 2 to 10 were used as a basis for the design of two test systems, one with low elastic follow-up and the other with a higher follow-up.

2.2 Design of experimental rigs

Two experimental rigs with different elastic follow-up factors were designed using the three bar concept shown in Figure 2; rig 1 to provide a target value of Z equal to about 2 and rig 2 with Z equal to about 6. These values are illustrated in Figure 4. The designs of the rigs were constrained by a number of practical features such as the available ceiling height in the creep laboratory and the dimensions of three-zone electric furnaces. An optimisation method, based on a genetic algorithm [15] was used to achieve the target values of elastic follow-up. The algorithm determined the diameters of the outer bars to achieve the target values of Z using constraints of furnace dimensions and ceiling height. The analysis also assumed the following; fixed dimensions for a modified C(T) specimen (initial crack length a_0= 19mm, specimen width , W=38mm and net section thickness B_n = 15mm), use of conventional cylindrical three-zone electric furnaces with a maximum internal diameter of 130 mm, allowing a clearance of 5mm between the side bars and the inside of the furnace, an overall height of the complete assembly of about 1m, ease of assembly of the rigs (this constrained the size of the nuts used to impose the residual stress), an ability to introduce known residual stress at high temperature without buckling the outer bars, and then applying a predetermined load to each test rig.

A schematic diagram of the final design is illustrated in Figure 5. The final overall heights of rig 1 and 2 were 740 and 865 mm respectively. The test rigs were designed to operate at 550°C and to

subject fracture mechanics specimens, manufactured from Type 316H stainless steel, to combinations of elastic follow-up, residual and applied loads.

Bars A and B were manufactured from Nimonic 80A and were screwed to rectangular top and bottom end sections, manufactured from EN24T steel. Four high temperature strain gauges (type ZFLA-3-11) were mounted on bars A and B at 90^0 intervals around their circumference to measure the applied strains and to determine the corresponding loads on the bars. Additionally a load cell was introduced to measure external loads applied to the rigs. The overall arrangement was fitted into a creep test frame so that an external load was applied to the assembly via a lever arm arrangement as illustrated in figure 5.

To measure the total displacement of the structure two linear voltage displacement transducers (LVDT) were mounted between the upper and lower sections. Also, capacitance gauges were fixed to the C(T) specimens to measure load line displacements. Seven thermocouples were used in the system to measure fracture specimen temperatures, temperatures at the positions of the strain gauges and the laboratory temperature. A direct current potential drop (PD) system was connected to the C(T) specimen to measure crack incubation and growth.

Initial designs for the experimental rigs involved using pins to transfer the load from the test rigs to each C(T) specimen. However, earlier experimental studies by Aird [16] showed that pin loading introduced significant changes in stiffness due to the presence of localized yielding between the pin and the specimen. To avoid this, the fracture specimens were modified to permit the specimen to be screwed directly to the Nimonic loading bars. A schematic of the revised C(T) specimen with locations for loading screws is shown in figure 6.

2.3 Introduction of residual stress

The experimental rigs were designed so that long range residual stress was introduced into the rig in a controlled manner. This was done by first connecting the Nimonic middle bars to the C(T) specimen and then screwing this completed assembly to the top and bottom end sections. The outer bars were then connected to the top end section and were free to move through the clearance holes in the bottom end section. All instruments were then connected to the test rig and the furnace, specimen and side bars, were heated to achieve 550°C for the C(T) specimen. This arrangement permitted free thermal expansion of the bars and the specimen. When a stable temperature was achieved, nuts S11 and S21 (shown in Figure 5) were loaded so that the top and bottom end pieces were forced apart. This resulted in bar A being loaded in tension and bars B subjected to balancing compressive forces. The force in each bar was determined from the strain gauge outputs. Finally, when the desired residual force was introduced into the structure (at high temperature), nuts S12 and S22 on bars B were tightened to the bottom end section.

Having introduced the desired residual force into the C(T) specimen, the entire assembly was then subjected to an applied load. The residual force in all three bars, crack mouth opening displacements (CMOD) of the C(T) specimens, potential drop readings and overall extensions of the rigs were recorded during the process.

3. Experimental studies

3.1 Sample preparation

An ex-service Type 316H stainless steel was used to manufacture fracture mechanics C(T) specimens. This material was provided as thick-walled pipes by EDF-Energy and identified as 2D2/2 (cast no. 55882). The chemical composition of the stainless steel is shown in Table 1. The ex-service material had seen about 72,000 hours operation at about 520°C. Eighteen specimens were extracted from thick walled pipes so that the cracks in the specimens were parallel to the radial direction. The specimens were manufactured according to ASTM 1457 [17] for pin loaded samples. Other specimens with a screw fitting arrangement, as shown in figure 5, were also manufactured. All C(T) specimens had cracks introduced by using wire electro-discharge machining and a wire diameter of 0.1 mm.

A summary of the dimensions of the specimens is given in Table 2. Three sets of specimens were prepared; a set for calibration studies (2 tests), a second set for creep incubation experiments using conventional constant load creep test rigs (12 tests) and a third set (4 tests) for use in the new experimental rigs. Of the conventional constant load tests, 5 tests (specimens BLP-01 to BLP-05) had been tested by Fookes [18] and Dean and Gladwin [19] and are included here for comparison. The remaining constant load specimens were tested in this programme and were a combination of pin-loaded C(T) specimens (ALP-01 to ALP-03) and screw-loaded C(T) specimens (ALS-01 to ALS-04). Finally the screw-loaded specimens for the elastic follow-up tests were AMS-01 and AMS-02 for rig 1 and AMS-03 and AMS-04 for rig 2.

The aim of the calibration studies was to establish whether the experimental rigs provided the target values of elastic follow-up. One millimetre diameter holes (notches) were introduced at the end of 0.1 mm wide cracks in specimens MC-01 and MC-02 and used to confine the non-linear behaviour of the C(T) specimen to local deformation and not crack growth. For the creep crack incubation tests the 0.1mm wide cracks were retained. All the specimens were then side grooved each side by 10 % of their thickness.

3.2 Calibration tests

A series of calibration tests were conducted and divided into two categories; preliminary stiffness tests on the components of the rigs and elastic-plastic load-unload tests using Type 316H stainless steel C(T) notched specimens MC-01 and MC-02 (shown in Table 2). All tests were carried out at 550°C.

The preliminary stiffness tests were conducted to obtain experimental values for the stiffness of bars and specimens. These results were then used to determine experimental values of elastic follow-up for the rigs. Loads were confined to low values so that material behaviour was elastic. First, only bar A with the screw loaded notched C(T) specimen was connected to both end sections. This was followed by heating the system to achieve 550^0C in the C(T) specimen. When a stable

temperature was reached external loads were applied to the middle bar via the lever arm arrangement and measurements of displacements and loads were made. The temperature profiles along the length of the various components of the rig were also measured. Data from this tests provided measured stiffness values for the series bar A and the C(T) specimen.

In a second stiffness test bars B were connected to the top and bottom end sections of each test rig with bar A and a notched C(T) specimen connected only to the top end section and free to move while the system was heated. Again, external loading was applied and measurements of displacements and loads were made. The results from these tests provided the stiffness of the outer bars, B.

In the second category of calibration tests the experimental rigs, containing notched C(T) specimens, were preloaded (i.e. residual force/stress was induced) then externally loaded to create elastic-plastic deformation in the C(T) specimen and unloaded to measure the relaxation of residual force. The extent of force relaxation depended on the elastic follow-up. First, a residual stress was introduced into the structure as discussed in earlier. Then the entire assembly was repeatedly loaded and unloaded to progressively higher load levels to induce elastic-plastic deformation in the notched C(T) specimens. The residual forces in all three bars, crack mouth opening displacements of the C(T) specimens, and overall extensions of the rig were recorded for both loading and unloading.

3.3 Creep crack incubation experiments

Two sets of creep crack incubation tests were carried out; conventional constant load tests using lever arm test machines and elastic follow-up tests using the new test rigs 1 and 2 (Figure 5). Each test specimen was heated within a three zone electric furnace. Conventional constant load tests were conducted using both pin and screw loaded C(T) specimens. Specimens ALP-01 to ALP-03, and specimens ALS-01 to ALS-04, shown in Table 2, were tested in this programme. Specimens BLP-01 to BLP-05 had been tested in earlier work, [18, 19]. The test samples (AMS -01 to 04), used in experimental rigs 1 and 2, were all screw loaded C(T) specimens.

In all tests the pre-loads and applied loads were devised to provide target values of reference stress, σ_{ref}, that were similar to those undertaken in earlier work [18]. A plane stress von-Mises reference stress was determined from [18]

$$\sigma_{ref} = \frac{P}{WB_n n_L} \tag{11}$$

where n_L is a normalised limit load function given by

$$n_L = \sqrt{(1+\gamma)\left(1+\gamma\left(a/W\right)^2\right)} - \left(1+\gamma\left(a/W\right)\right) \quad \text{with} \quad \gamma = 2/\sqrt{3} \tag{12}$$

The loads required to achieve the target values of reference stress for constant load specimens are shown in Table 3a. The elastic follow-up tests in rigs 1 and 2 each had samples subjected to combinations of misfit and applied loads to achieve initial total reference stresses of 280 and 240 MPa. These loads are shown in Table 3b. For the tests in rig 1 the target values of misfit or initial force in specimens AMS-01 and AMS-02 gave rise to misfit reference stresses of about 180MPa. For tests in rig 2, specimens AMS-03 and 04 the misfit reference stress was about 130MPa.

Capacitance gauges were mounted on the C(T) specimens to measure crack mouth opening displacements. Direct current potential drop was used to measure onset of crack incubation and growth. The duration of each test is shown in Table 3. Once the tests were stopped and unloaded the specimens were sectioned to measure final crack lengths and to examine the details of crack extension from the initial EDM starter notches.

4. Results and Discussion

4.1 Estimates of elastic follow-up from system stiffness

Theoretical values of the elastic follow-up Z of the two test rigs were calculated using equations 2 to 9. To do this it was necessary to determine an average Young's modulus for bars A and B. This was because different sections of the three bar system were exposed to different temperatures when the C(T) specimen was maintained at 550^0C. From the temperature profile an average Young's modulus [20] was calculated to provide values of stiffness of the various elements of the system shown in Figure 5. Irrespective of whether the specimens were screw loaded rather than pin loaded in the two test rigs the specimen stiffness was determined from equation 4 assuming an initial crack length of 19.5mm. Theoretical values obtained from the analysis are given in Table 4.

Experimental values of elastic follow-up were calculated from data provided from the preliminary tests. The stiffness of each C(T) specimen at high temperature was obtained from the slope of the measured crack mouth opening displacements (CMOD) as a function of the applied load (measured by the system load cell). The stiffness of bar A (Figure 2) was determined again from the slope of the total measured displacement (with the CMOD subtracted) as a function of the applied load. Data from tensile tests conducted on side bars B in the elastic region (at 550°C) were used to calculate the stiffness of the side bars. The loads acting on each bar were calculated using strain gauges mounted on the bars and the displacement measured from LVDTs shown in Figure 5. Experimental values of stiffness of the elements of the system are given in Table 4 together with the corresponding values of elastic follow-up.

Experimental values of the stiffness of the screw loaded C(T) specimens were found to be higher than the theoretical values. However, this was balanced by lower experimental values of bar A for each test rig, giving lower values of the experimental effective stiffness for bar A and screw loaded C(T) specimen in each test rig compared to theoretical values. This results in the experimental stiffness ratio β being lower than predicted values. Overall the experimentally evaluated elastic follow-up provided by the system to the screw loaded C(T) specimen in each test rigs matched the theoretical values within about 10%. Experimental values of Z are shown in Figure 4.

4.2 Estimates of elastic follow-up from repeated load-unload tests

The preloaded high temperature tests, using the notched and screw loaded C(T) specimens MC-01 and -02, subjected to repeated loading and unloading (to zero applied load), provided results shown in Figure 7. In each test the specimens were preloaded (through elastic misfit) to introduce a nominally identical residual force (about 6.3KN). This is point A in Figure 7. The application of additional external loading led to elastic-plastic deformation occurring in the notched C(T) specimen. On subsequent unloading the initial residual force had been reduced since the accumulated plastic deformation had accommodated the initial elastic misfit. For example, as a result of repeated loading and unloading on specimen MC-01 in test rig 1, the initial tensile residual force in middle bar relaxed from 6.25 kN to 2.83 kN (point B in Figure 7a) while the average compressive residual force in the side bars relaxed from 3.14 kN to 1.43 kN. Similar load-CMOD characteristics were exhibited during testing of specimen MC-02, as shown in Figure 7b. The line AB in Figure 7a and b corresponds to the locus of unloaded points (at zero applied load) and revealed that the relaxation of the initial residual stress was proportional to the degree of plastic CMOD accumulated in each specimen.

An important feature of the behaviour of both test assemblies is that the relaxation line AB has a slope dependent on the relative stiffness of the assembly and in turn corresponded to the elastic follow-up associated with the structure. The initial preload relaxed more in the rig with low elastic follow-up compared to the rig with high follow-up. The locus of points for the relaxation of the initial residual force was approximately linear and the elastic follow up was determined using an approach developed by Smith et al [6]. The elastic follow-up, Z_R , estimated from relaxation of the initial residual force in the specimen, is obtained from the ratio of the CMOD at points A, B and C, shown in Figure 6a. Z_R is given by

$$Z_R = \frac{CMOD_B - CMOD_C}{CMOD_A - CMOD_C} \tag{13}$$

This equivalent to the definition for Z provided by equation 1. Values for Z_R for rigs 1 and 2 obtained from figure 7a and b were 2.15 and 12. The experimental result from the repeated load-unload tests in test rig 1 is similar to both the theoretical and experimental values obtained from the relative stiffness of the elements of the system. These values are given in Table 4. In contrast Z_R for rig 2 was higher than the estimates given in Table 4.

4.3 Creep deformation and elastic follow-up

For the specimens subjected to creep deformation, selected experimental load versus crack mouth opening displacements of some of the C(T) specimens are shown in Figure 8. Constant load test data for specimens ALS-02 and ALS-03 (at initial reference stresses of 280 and 240MPa respectively) are compared in Figure 8a with specimens AMS-03 and AMS-01 (both subjected to initial reference stresses of 280MPa). Figure 8b compares test results for specimens AMS-02 and AMS-04 with ALS-03, all of which had initial reference stresses of 240MPa.

All specimens experienced significant plastic deformation prior to creep. As observed by Fookes and Smith [10] this is a feature of the behaviour of Type 316H stainless steel when specimens are subjected to reference stresses in excess of the yield strength (172MPa at 550°). Notably during initial loading of specimens with elastic follow-up the creation of plastic deformation in the specimens led to elastic follow-up and initial relaxation of the initial misfit and total forces on the specimens prior to creep. This is particularly evident in Figures 8a and b for specimens in test rig 1, AMS-01 and -02. The target reference stresses of 280m and 240MPa could not be attained due to plastic relaxation of the misfit force. For example the initial misfit force in specimen AMS-01 reduced from 9.38KN to 8.04KN.

Relaxation of the specimen forces in the four elastic follow-up tests, illustrated in Figures 8a and b, were accompanied by increasing amounts of crack mouth opening displacement. Unlike a constant displacement controlled test the increasing CMOD was caused by elastic follow-up in the system. The elastic follow-up in rig 1, with Z ~ 2, led to significant load relaxation for specimens AMS-01 and 02. For the former specimen, the initial misfit load had relaxed in Figure 8a from point A at 8.04 KN to point B at zero load with the initial total force relaxing from point A' at 14.53 KN to point B' at 4.62 KN. Similar behaviour was observed for specimen AMS-02 as shown in Figure 8b, with points A and A' corresponding to the initial misfit and total loads, and points B and B' the final misfit and total loads on the specimen.

For rig 2 with Z ~ 7 there was less load relaxation, with the misfit and total loads, shown in Table 3b, relaxing between 6 and 12% by the end of the tests. The extent of load relaxation and elastic follow-up for specimens AMS-03 and -04 can be seen in Figure 8.

The relaxation of the total reference stresses for three experiments, ASL-03, AMS-01 and AMS-04 are shown in Figure 9. The reference stress in each case was calculated assuming there was no crack extension. Similar to the specimen load results shown in Figure 8, there was only limited reference stress relaxation for specimen AMS-04, while specimen AMS-01 exhibited significant relaxation of the specimen reference stress.

Estimates of the elastic follow-up during stress relaxation of the four tests AMS-01 to 04 were determined in a manner similar to that for plastic deformation induced in the repeated load-unload tests MC-01 and 02. Referring to Figure 8a), where lines A-B and C-B are parallel to lines A′-B′ and C′-B′ respectively, experimental values of Z_{exp} for each test were determined from

$$Z_{exp} = \frac{CMOD_{B\prime} - CMOD_{C\prime}}{CMOD_{A\prime} - CMOD_{C\prime}} = Z_R = \frac{CMOD_B - CMOD_C}{CMOD_A - CMOD_C} \quad (14)$$

Values of elastic follow-up determined using equation 14, using data from tests AMS-01 to -04 are shown in Table 5. Also shown in Table 5 are the earlier theoretical and experimental results. It is notable that the values Z for the creep elastic follow-up tests are consistently lower than estimates

provided by theory, experimental stiffness measurements and from the elastic-plastic tests MC-01 and MC-02.

4.4 Creep crack incubation

At constant load the C(T) specimens continued to deform and cracks eventually initiated ahead of the initial EDM notch in the specimens. A typical micrograph obtained from a section extracted from the mid-thickness of specimen ALS-02 is shown in Figure 10. This revealed a final crack extension of about 0.8mm for a test duration of 541 hours. The cracking was found to be intergranular and essentially identical to that found in earlier work Fookes [10, 18], (specimens BLP-01 to -05 in Table 3). The final measured crack extensions were used to calibrate the voltage change obtained from the direct current potential drop system. Crack incubation times corresponding to 0.03, 0.1 and 0.2mm crack extension were then determined. These times are shown in Figure 11 as a function of the initial applied reference stress, with results from pin-loaded specimen exhibiting a similar logarithmic trend to those from screw-loaded specimens. Nevertheless, the screw loaded specimens exhibited shorter incubation times at relatively low reference stresses compared to the pin-loaded specimens. Irrespective of these differences, collated data were fitted with power law expressions for different amounts of crack growth. The crack incubation time, $t_i[\Delta a]$, was assumed to be given by

$$t_i[\Delta a] = A(\sigma_{ref})^b \tag{15}$$

where A and b are fitted constants and σ_{ref} is the initial reference stress at the initial crack length. Fitted curves are given in Figure 10 with the constants A and b given in Table 6. The slopes of the curves are approximately the same but the slope, b, becomes slightly less negative as the crack extension becomes larger.

The mode of crack growth was intergranular in the four elastic follow-up tests and identical to the constant load tests. Micrographs of two of the tests shown in Figure 10. The crack incubation times for the four elastic follow-up tests are shown in Figure 11 corresponding to crack increments of 0.03mm. All results are shown for incubation times based on the initial total reference stress. Also indicated are the final relaxed reference stresses for the four elastic follow-up tests. The key feature of these results is that for the same initial reference stress the crack incubation times were significantly larger compared to constant load. Notably results for specimens in test rig 1 with Z~2 the incubation times were the greatest, with the Z~7 tests intermediate between the load controlled data and Z~2 data. As expected the greater the stress relaxation and lower the elastic follow-up the longer the incubation time. Figure 12 shows that the incubation times, based on the final relaxed references stresses, for the Z ~ 7 tests lie closer to the constant load times. In contrast, if the final relaxed stress in the Z ~ 2 tests were used to estimate the crack incubation time (based on the constant load results) the predicted incubation times would be well in excess of those observed.

Figure 13 shows the results from the elastic follow-up tests, again in terms of the initial total reference stress, but for crack increments equal to 0.1 mm. Once more, all elastic follow-up incubation data lie at times greater than the constant load tests for the same initial reference stress.

In addition to the results shown in terms of reference stress in Figures 12 and 13 a fracture mechanics approach was adopted. A material toughness was calculated using procedures developed in earlier work [10] with the toughness $K_{mat}[\Delta a]$, corresponding to the increment of crack growth from the initial notch, given by

$$K_{mat}[\Delta a] = \sqrt{E' J_{mat}[\Delta a]} \tag{16}$$

where $E' = \frac{E}{1-\nu^2}$ and J_{mat} is given by [21]

$$J_{mat}[\Delta a] = \frac{\eta U_T}{B_n(W-a_0)} \tag{17}$$

For a C(T) specimen

$$\eta = 2 + 0.522(1 - \frac{a_0}{W}) \text{ for } 0.45 \leq \frac{a_0}{W} \leq 0.7 \tag{18}$$

U_T is the area under the load-crack mouth opening displacement curves including the elastic, plastic and creep displacements. It was assumed that η was the same for both pin and screw loaded C(T) specimens. Equations 16 to 18 were evaluated for all specimens shown in Table 3 and the corresponding initiation times for crack extension of 0.03mm as a function of K_{mat} are shown in Figure 14. In the case of the constant load tests and similar to decreasing reference stresses leading to longer incubation times, results in Figure 14 show that for longer incubation times the material toughness decreases, i.e. the slope in Figure 14 is negative. This is similar to the relationships between material toughness and creep crack incubation times shown in other work on steels tested at high temperature [22].

As with the results in terms of reference stress illustrated in Figure 12 the combined loading and elastic follow-up tests results in Figure 14 show longer crack incubation times for the same values of K_{mat} achieved for load control tests. However, the microstructural evidence in Figure 10 indicates that there was not a change in the mechanism of creep crack incubation between constant load tests and combined loading tests. Therefore it is unlikely that the intrinsic material toughness for a given incubation time was different for different loading conditions. This suggests two aspects; first, unlike load control conditions, not all the available strain energy provided in combined loading was dissipated to generate creep damage leading to creep crack incubation. Rather, creep deformation led to load relaxation and the degree of elastic follow-up dictated the rate of relaxation. Second, to calculate material toughness all the dissipated strain energy was included in equation 17 to calculate material toughness. If strain energy was dissipated in load relaxation rather than contributing to creep damage accumulation then equation 17 overestimates the

material toughness. Consequently, the current methods for determining material toughness for creep crack incubation in laboratory specimens are not adequate for combined loading conditions.

5. Concluding remarks

The test rigs created in this research provided loading conditions for fracture mechanics specimens that lay between constant load and constant displacement. The test rigs were also designed so that initial misfit long range residual stresses could be introduced in combination with applied stresses. These experiments differ from earlier approaches [8-10] where self-equilibrating residual stresses were introduced directly into fracture mechanics specimens.

Experiments in the new test rigs provided measured values of elastic follow-up. It was found that the values obtained were not consistently the same as those provided by theory. In particular, it was found that the experimental values of follow-up were lower than predicted.

The new test rigs were able to provide experimental creep crack incubation times (corresponding to different amounts of crack extension) in the presence of elastic follow-up and with combined residual and applied stresses. In parallel, creep crack incubation times were obtained from conventional load controlled tests. For the four tests using the new test rigs it was demonstrated that longer incubation times were attained compared to constant load tests. Tests with elastic follow-up illustrated that there was relaxation of the total and the initial misfit forces on the test specimens. Tests having low values of elastic follow-up ($Z \sim 2$) resulted in significant relaxation of the initial residual forces and considerable increases in the creep crack incubation time. Tests with $Z \sim 7$ again exhibited longer incubation times, but at lower levels of residual force relaxation the incubation times were shorter than for $Z \sim 2$.

The mechanism for crack incubation between constant load and combined loading tests was the same. Therefore, material toughness measured from the two types of tests would be expected to be the same. However, measured toughness for the same incubation time from combined loading tests was higher than for constant load tests. Further work will explore models for predicting the relaxation of initial residual forces in the presence of elastic follow-up and their contribution to creep crack incubation.

Acknowledgments

The authors gratefully acknowledge the financial support provided by EDF Energy for this research. Additionally, David Smith is also supported by the Royal Academy of Engineering, EDF-Energy and Rolls-Royce plc.

References

[1] Coleman, M.C., Miller, D.A., Stevens, R.A., Reheat cracking and strategies to assure integrity of Type 316 weld components. In: Proceedings of the International Conference on Integrity of High Temperature Welds. London: PEP Ltd.; 1998, 169–79.

[2] Smith, D.J., Bouchard, P.J., and George, D., Measurement and prediction of residual stresses in thick-section steel welds, J Strain Analysis, 2000, 35, 287-305

[3] Roche. R.L., Modes of failure - primary and secondary stresses. In American Society of Mechanical Engineers Pressure Vessels and Piping Conference, 1987, 171–176,

[4] Boyle, J. T., and Nakamura, K., The assessment of elastic follow-up in high temperature piping systems – overall survey and theoretical aspects. International Journal of Pressure Vessels and Piping, 1987, 29, 167–194.

[5] Kasahara, N., Strain concentration at structural discontinuities and its prediction based on characteristics of compliance changes in structures, JSME Int Jnl Series A, Solid Mechanics and Materials Engineering, 2001, 44(3), 354-361

[6] Smith, D. J., McFadden, J., Hadidimoud, S., Smith, A. J., Stormonth Darling, A. J., and. Aziz, A. A., Elastic follow-up and relaxation of residual stresses, Proceedings of the Institution of Mechanical Engineers Part C: Journal of Mechanical Engineering Science, 2010, 224, 777–787

[7] Aird, C.J., Hadidimoud, S., Truman, C.E., Smith, D.J., Impact of residual stress and elastic follow-up on fracture", Journal of ASTM, 2008, 5 (8). JAI101608

[8] Webster, G. A. and Ainsworth, *High Temperature Component Life Assessment,* Chapman and Hall, Cambridge, England, 1994

[9] Ainsworth, R. A., The Use of Failure Assessment Diagram for Initiation and Propagation of Defects at High Temperature. *Fatigue Fract. Engng Mater. Struct*, 1993, **16**, 1091-1108.

[10] Fookes, A., and Smith, D.J., "A new method for assessing high temperature crack growth", Fatigue Fract Engng Mater Struc, 2005, **28**, 769–778.

[11] Turski, M., Bouchard, P.J., Steuwer, A. and Withers, P.J. Residual stress driven creep cracking in {AISI} type 316 stainless steel. Acta Materialia, 2008, 56(14):3598 – 3612

[12] O'Dowd, N. P., Nikbin, K. M., Wimpory, R. C., Biglari, F. R. and ODonnell, M. P., Computational and experimental studies of high temperature crack initiation in the presence of residual stress, Journal of Pressure Vessel of Technology, 2008, 130, 31–37

[13] Hossain, S., Truman, C. E., and Smith, D. J., Generation of residual stress and plastic strain in a fracture mechanics specimen to study the formation of creep damage in type 316 stainless steel, Fatigue & Fracture of Engineering Materials & Structures, 2011, 34, 654–666

[14] Anderson, T.L., *Fracture mechanics - fundamentals and applications",* Taylor and Francis, 2005.

[15] Goldberg, D.E., "Genetic algorithms in search, optimisation and machine learning", Pearson Education, 2004.

[16] Aird, C. J., *"The influence of long-range residual stress on the cleavage fracture of ferritic steel"*, PhD thesis, University of Bristol, 2009.

[17] American Society for Testing and Materials, *"Standard test method for measurement of creep crack growth rates in metals"*, ASTM E1457-00, 2000.

[18] Fookes, A. J., Assessment of crack growth in steels at high temperature. PhD thesis, University of Bristol, 2003.

[19] Dean, D.W. and Gladwin, D. N., Creep crack incubation and growth behaviour of type 316h steels. Technical report, British Energy Generation, Limited E/REP/BDBB/0040/GEN/03, April 2004.

[20] Special Metals. Nimonic alloy 80A. Technical report SMC-099, September 2004, http:/www.specialmetals.com/documents/Nimonic%20alloy%2080A.pdf

[21] European Structural Integrity Society. ESIS procedure for determining the fracture behaviour of materials. ESIS P2-92, 1992

[22] Mueller, F., Scholz, A. and Berger, C., Comparison of different approaches for estimation of creep crack initiation, Engineering Failure Analysis 2007, 14, 1574–1585.

Table 1. Chemical composition of the 316H stainless steel

Chemical	C	Mn	Si	P	S	Cr	N	Mo	Al	Ti	W	V	Co	Cu
Weight (%)	0.04	1.49	0.29	0.02	0.014	17.1	11	2.38	<0.005	0.013	0.042	0.02	0.09	0.09

Table 2. Specimen details

Test type	Test ID	W (mm)	B (mm)	B_n (mm)	a_0 (mm)
Calibration tests	MC-01	37.91	19.10	15.46	19.47
	MC-02	37.90	19.11	15.46	19.48
Constant load creep crack incubation tests	ALP-01	38.01	19.04	15.01	19.57
	ALP-02	37.99	19.14	15.12	19.42
	ALP-03	37.99	19.14	15.18	19.49
	ALS-01	38.01	19.12	15.12	19.44
	ALS-02	38.01	19.12	15.88	19.54
	ALS-03	38.07	19.12	15.83	19.30
	ALS-04	37.97	19.13	15.92	19.23
	BLP-01	*37.91*	*18.85*	*15.27*	*20.68*
	BLP-02	*38.01*	*18.92*	*15.62*	*20.03*
	BLP-03	*37.90*	*18.98*	*15.59*	*20.14*
	BLP-04	*37.97*	*18.98*	*15.50*	*19.79*
	BLP-05	*37.82*	*19.02*	*15.56*	*19.94*
Mixed loading creep crack incubation tests	AMS-01	37.99	19.13	15.86	19.27
	AMS-02	38.05	19.03	15.38	19.59
	AMS-03	37.80	19.09	15.46	19.36
	AMS-04	37.83	19.04	15.36	19.36

Specimens BLP-01 to BLP-05 were tests undertaken by Fookes [18] and Dean and Gladwin [19]

Table 3 Summary of constant load and elastic follow-up tests

a) Constant load tests

Test ID	Applied force (kN)	Specimen reference stress, MPa	Final CMOD (mm)	Final crack extension Δa (mm)	Test duration (hours)
ALP-01	13.33	281	0.094	0.857	425
ALP-02	16.35	336	0.310	0.959	96
ALP-03	13.24	336	0.491	1.623	141
ALS-01	16.40	338	0.393	1.070	151
ALS-02	14.11	280	0.136	0.848	541
ALS-03	12.46	240	0.058	0.882	1508
ALS-04	9.40	180	0.049	0.637	4583
BLP-01	*7.86*	*184*	*0.136*	*2.97*	*16630*
BLP-02	*10.17*	*215*	*0.173*	*2.63*	*4698*
BLP-03	*12.83*	*282*	*0.235*	*1.242*	*1921*
BLP-04	*13.68*	*288*	*0.257*	*1.423*	*1589*
BLP-05	*15.50*	*336*	*0.299*	*0.90*	*171*

b) Elastic follow-up tests

Test Rig	Test ID	Initial forces on specimen at start of test $F_S^{Initial}$ (kN)		Total Force on specimen at start of test (kN)	Total specimen reference stress at start of test, (MPa)	Final forces on specimen at end of test F_S^{Final} (kN)		Total force on specimen at end of test KN	Final CMOD (mm)	Final crack extension Δa (mm)	Test duration (hours)
		F_S^R	F_S^A	F_S^{Total}	σ_{ref}	F_S^R	F_S^A	F_S^{Total}			
1 (Z~2)	AMS-01	9.38 (8.04[1])	5.15	14.53 (13.19[1])	280 (254)	0	4.62	4.62	0.330	0.107	3816
1 (Z~2)	AMS-02	8.91 (8.28[1])	2.79	11.70 (11.07[1])	240 (227)	2.48	2.79	5.27	0.260	0.030	4883
2 (Z~7)	AMS-03	6.33	7.65	13.98	280	4.63	7.65	12.28	0.420	0.887	3096
2 (Z~7)	AMS-04	6.36	5.43	11.79	240	5.54	5.43	10.97	0.265	0.169	4229

F_S^R : Residual force, F_S^A : Applied force , [1]Force at the end of applied load

Table 4 Comparison of element stiffness and elastic follow up for each test rig

Test Rig 1	k_s N/mm	k_A N/mm	k_B N/mm	k_{eff} N/mm	β	α_{eff}	Z_s	Z_{eff}	Z
Theoretical	70322	145612	79850	47421	2.071	3.368	1.483	1.297	1.923
Experimental	79153	104791	99582	45093	1.324	4.417	1.755	1.226	2.153

Test Rig 2	k_s N/mm	k_A N/mm	k_B N/mm	k_{eff} N/mm	β	α_{eff}	Z_s	Z_{eff}	Z
Theoretical	70145	19924	18814	15516	0.284	2.425	4.521	1.412	6.385
Experimental	73826	17242	17898	13978	0.234	2.562	5.282	1.39	7.344

Table 5 Theoretical and experimental values of elastic follow up for each test rig

Condition	**Test rig 1**	**Test rig 2**
Theoretical	1.923	6.385
Experimental –derived from measured stiffness	2.153	7.344
Experimental elastic-plastic MC-01	2.15	-
Experimental elastic plastic MC-02	-	12
Experimental elastic-plastic-creep AMS-01	1.35	
Experimental elastic-plastic-creep AMS-01	1.27	
Experimental elastic-plastic-creep AMS-01	-	4.73
Experimental elastic-plastic-creep AMS-01	-	4.29

Table 6 Creep crack incubation constants A and b derived from tests using pin and screw loaded C(T) specimens

Crack increment, Δa, mm	**A**	**b**
0.03	5.83×10^{17}	-6.56
0.10	4.07×10^{16}	-5.90
0.20	2.04×10^{16}	-5.68

Units of stress in MPa, time in hours

Figures

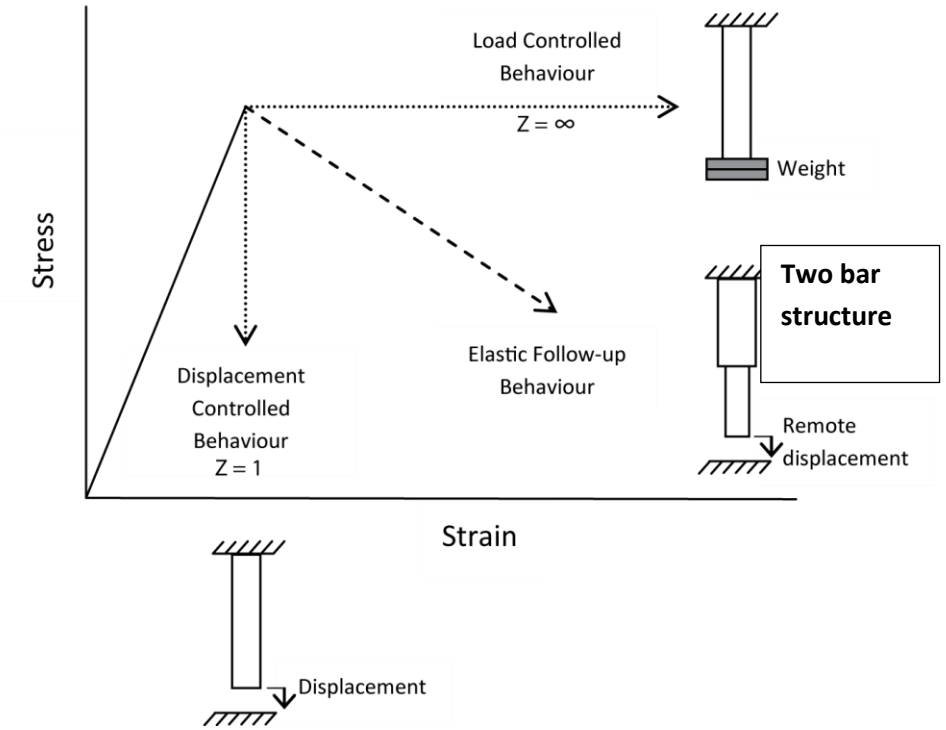

Figure 1 Stress-strain behaviour of a local volume undergoing non-linear behaviour for different loading conditions

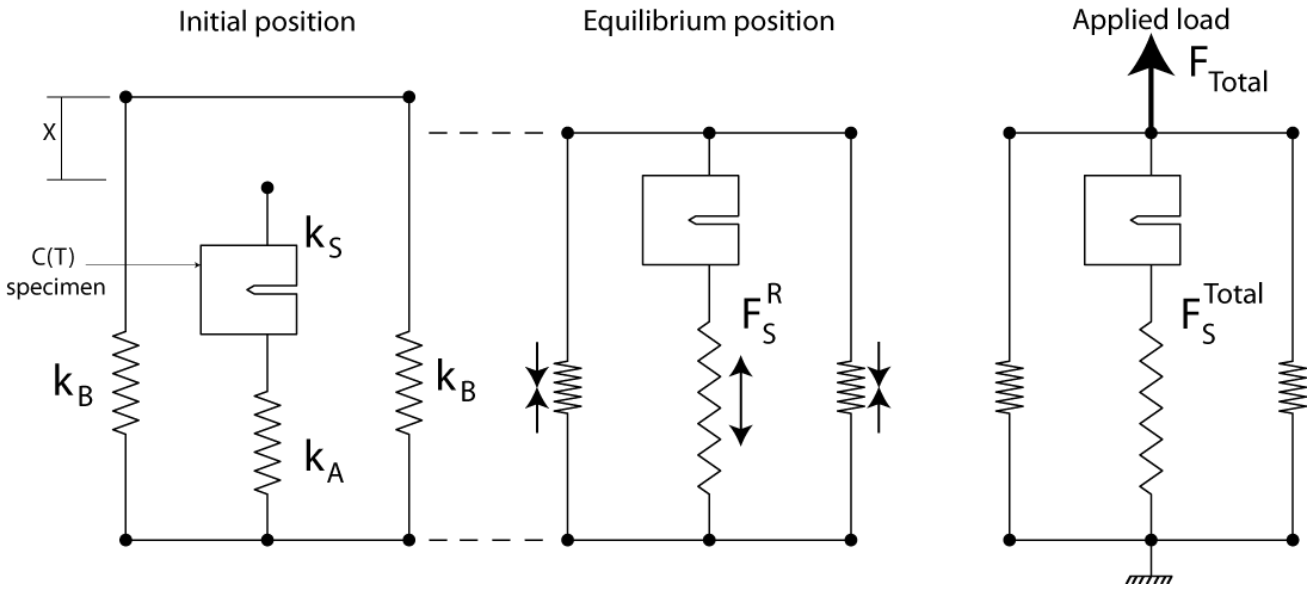

Figure 2 Three bar loading system for introducing combined residual and applied forces.

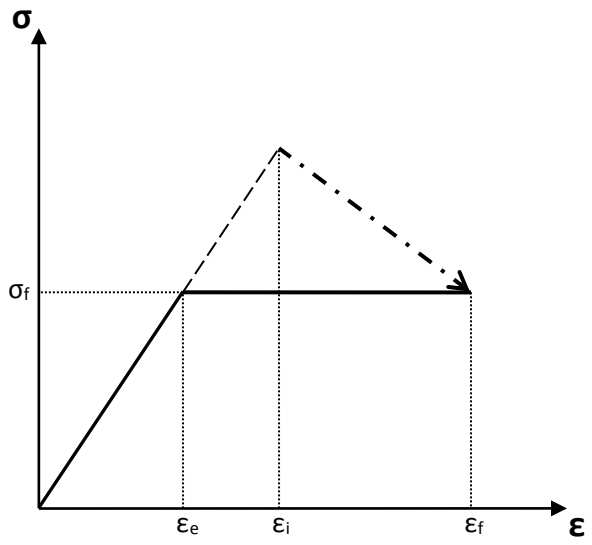

Figure 3 Idealised elastic-plastic response of fracture specimen in a three bar assembly (σ=reference stress, ε=reference strain)

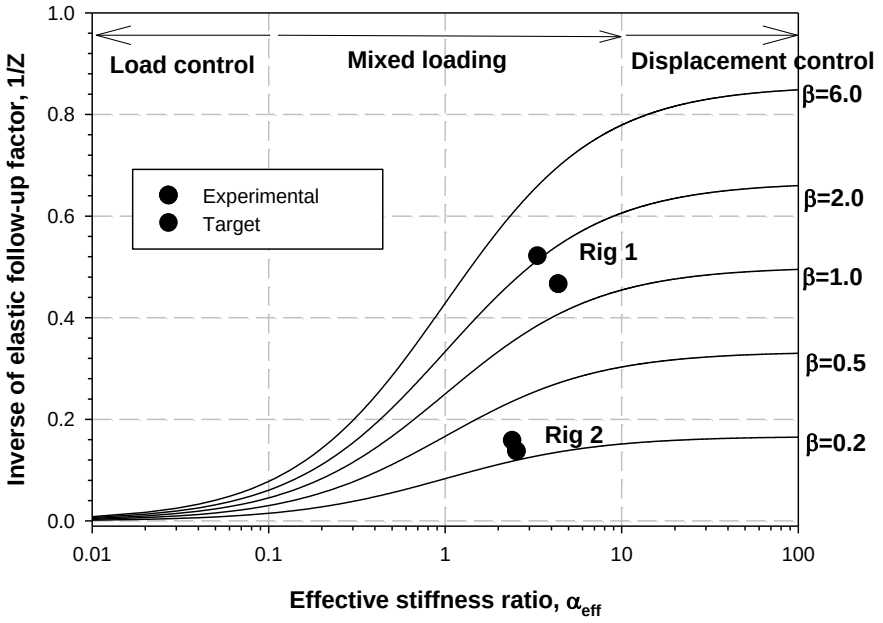

Figure 4 Variation of elastic follow-up in a three bar structure, illustrating target and experimental values for Rigs 1 and 2

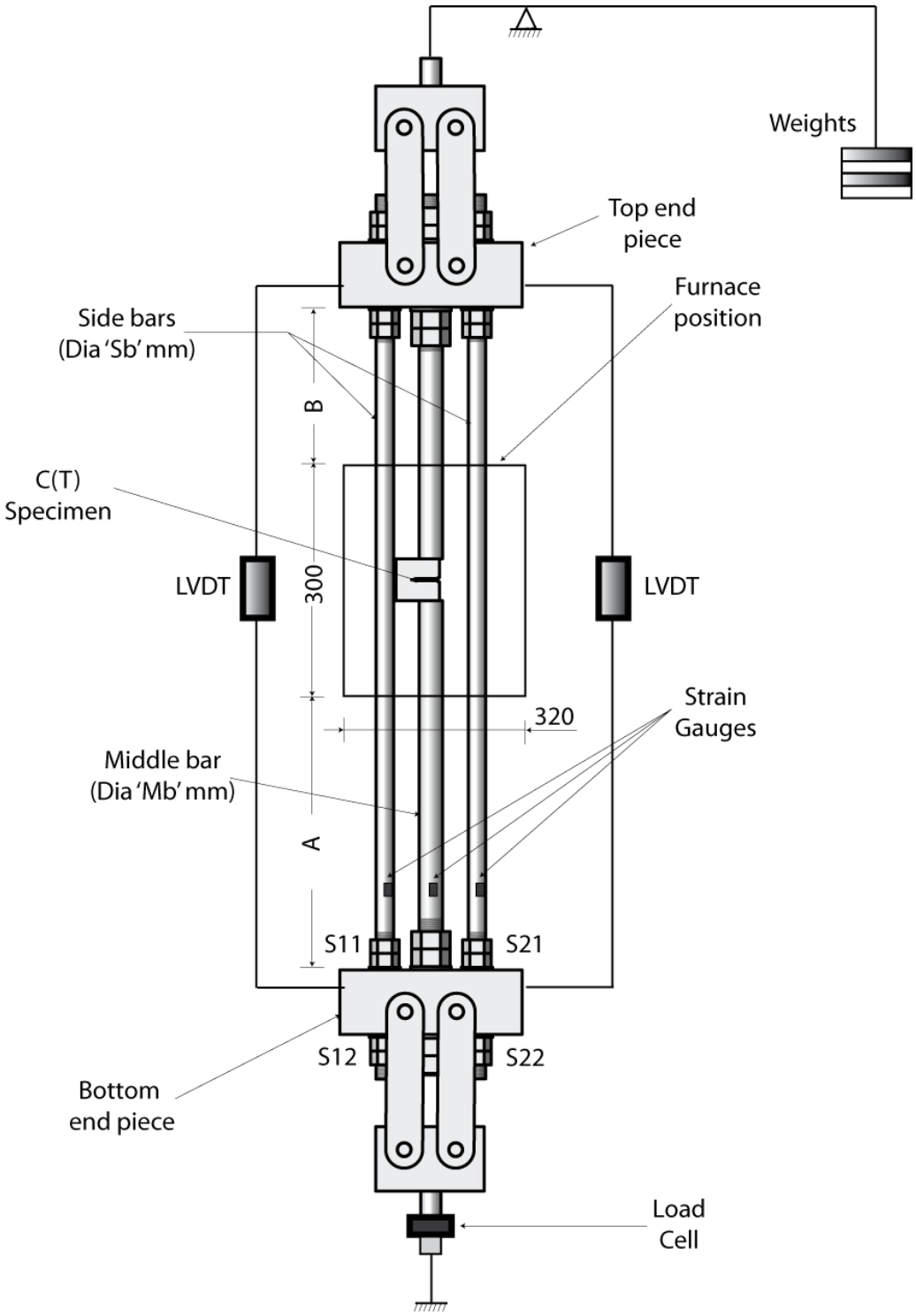

Rig No.	Dimensions (mm)			
	A	B	Sb	Mb
1	312	128	19.62	25.61
2	347	218	10.00	10.00

Figure 5 Schematic of experimental three bar assembly (All dimensions in mm)

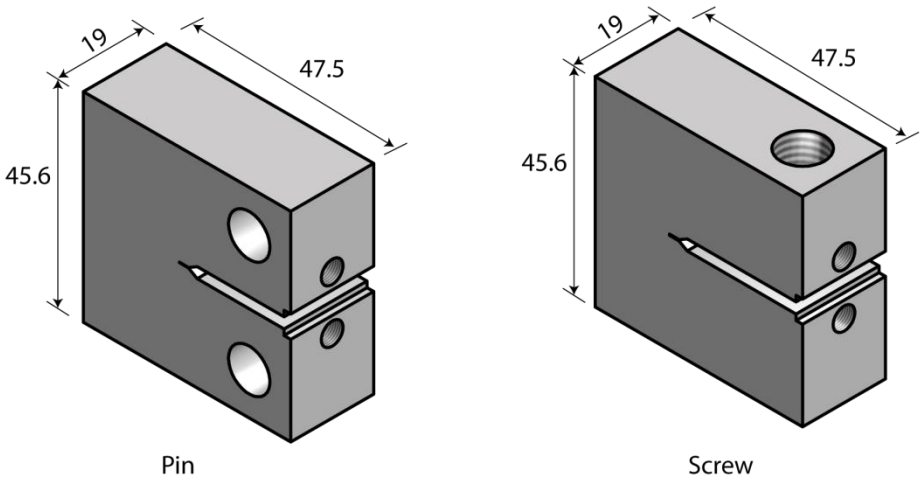

Figure 6: Schematic of pin-loaded and screw-loaded C(T) specimens. (All dimensions in mm)

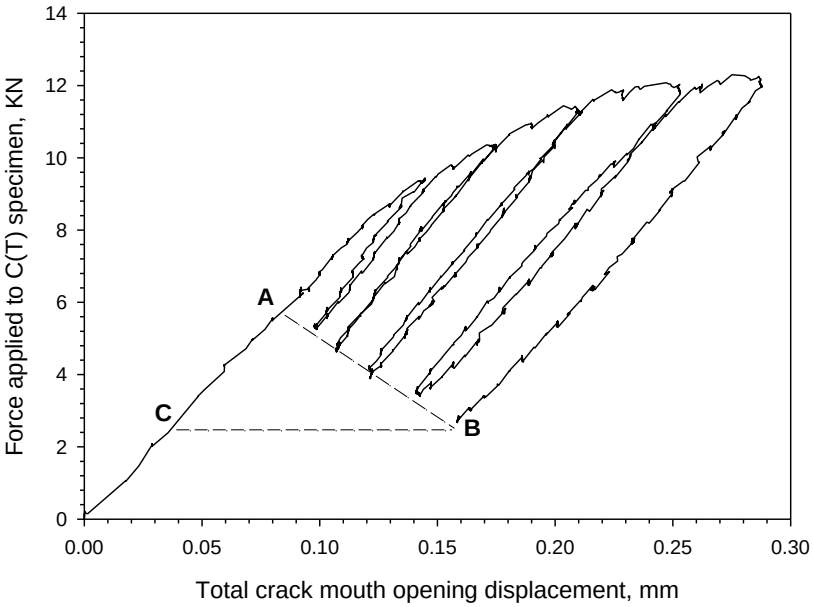

(a)

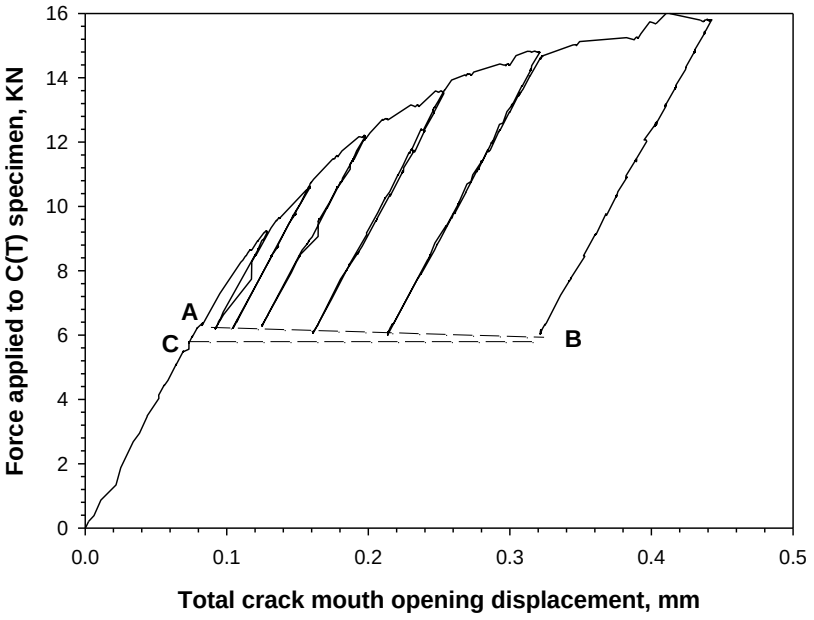

(b)

Figure 7: Repeated load-unload behaviour of Type 316H stainless steel C(T) specimens within two different elastic follow-up test rigs at 550°C, a) test rig 1 with Z ~ 2, b) test rig 2 with Z ~ 7. Points A, B and C determine the degree of elastic follow-up

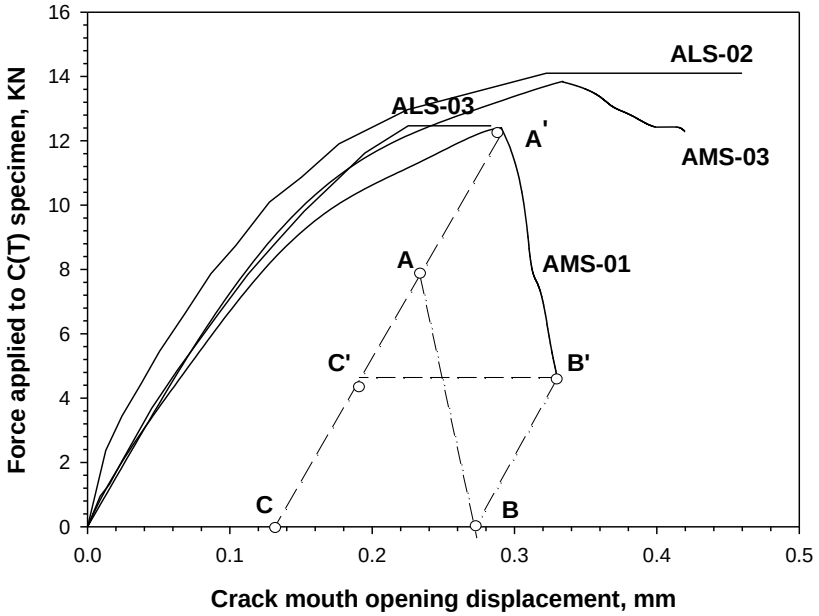

a) Tests ALS-02, ALS-03, AMS-01 (Z ~ 2) and AMS-03 (Z ~ 7)

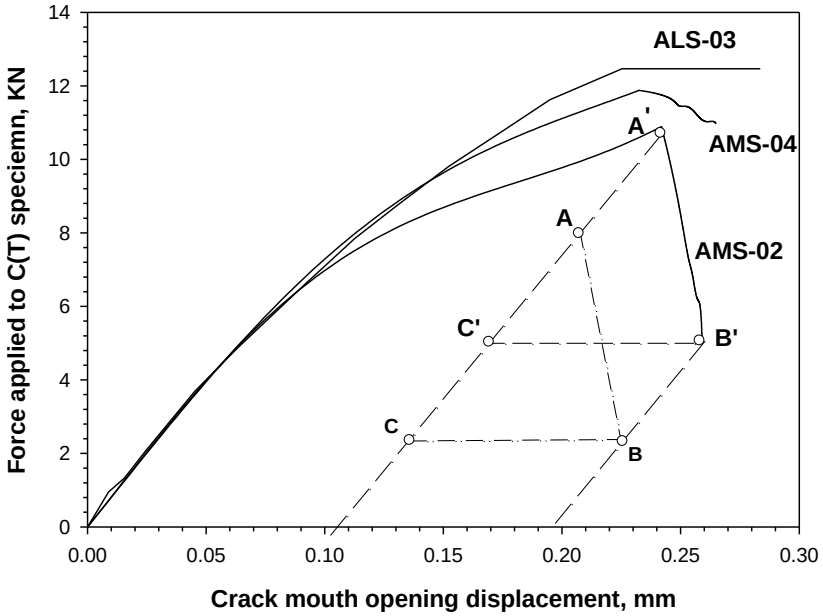

b) tests ALS-03, AMS-02 (Z ~ 2) and AMS-04 (Z ~ 7)

Figure 8 Load and crack mouth opening response of Type 316 H stainless steel C(T) specimen at 550°C. Specimens ALS-02 and ALS-03 were conventional load controlled. Specimens AMS-01 to 04 were combined residual and applied load tests with elastic follow-up.

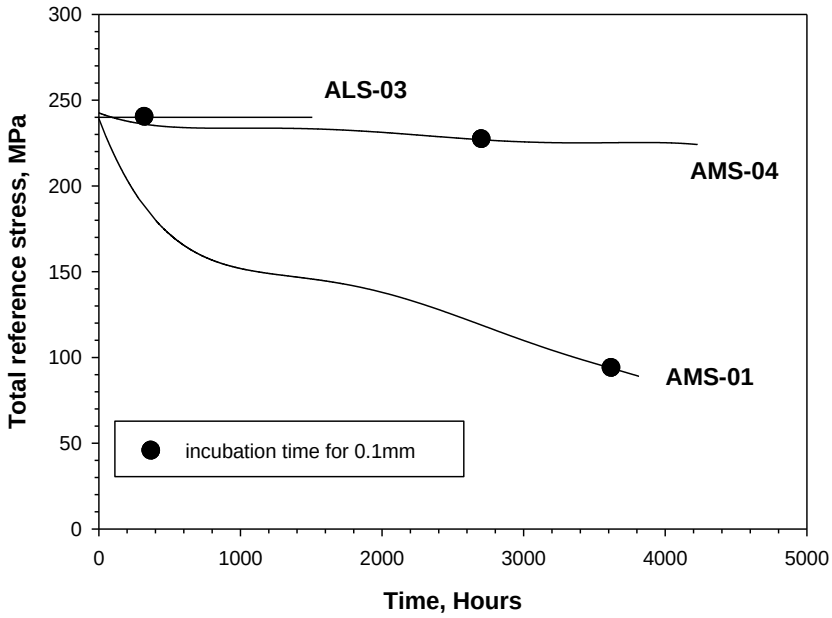

Figure 9: Variation in reference stress during tests ALS-03, AMS-01 and AMS-04. Values of the incubation time for crack extension of 0.1mm are shown.

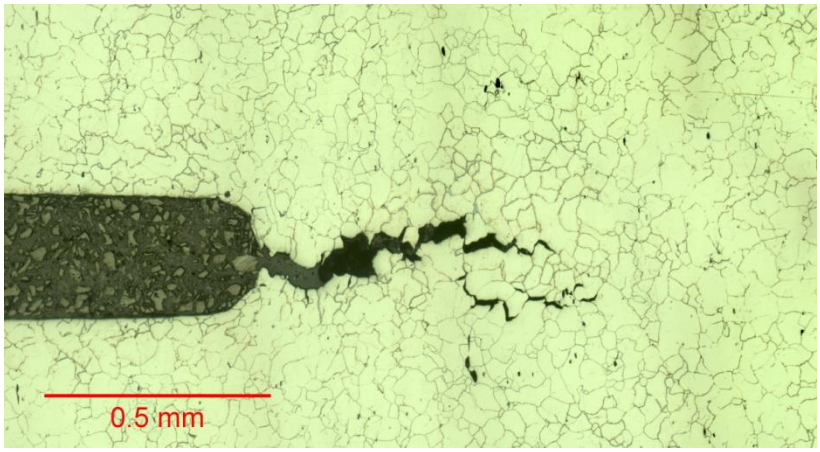

(a) ALS-02

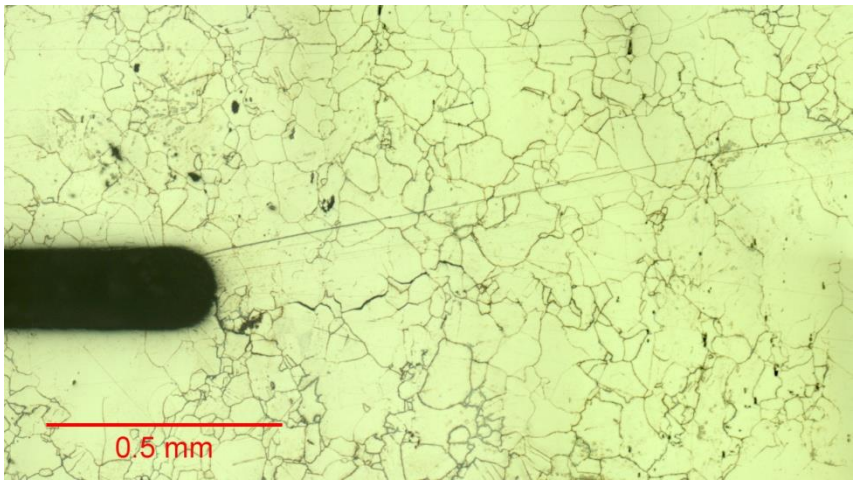

(b) AMS-01

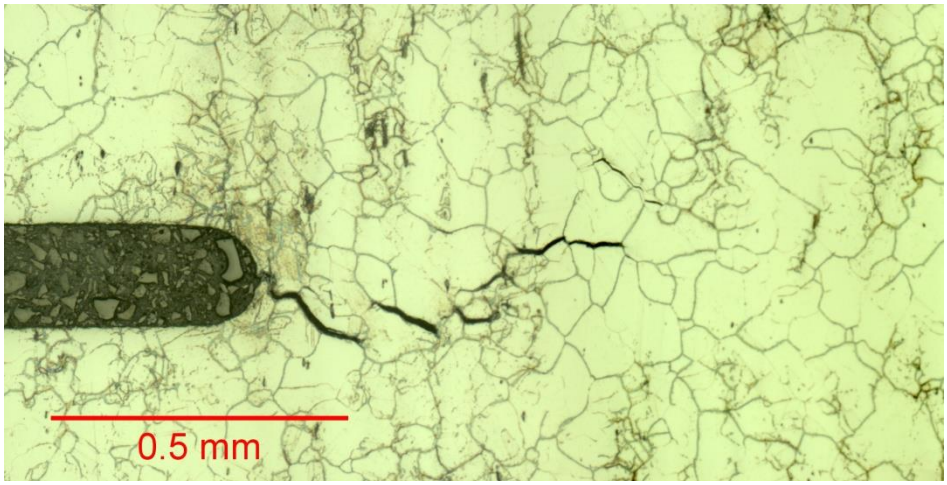

(c) AMS-03

Figure 10 Polished and etched micrographs from sections extracted from mid-thickness of selected C(T) specimens after testing at 550°C

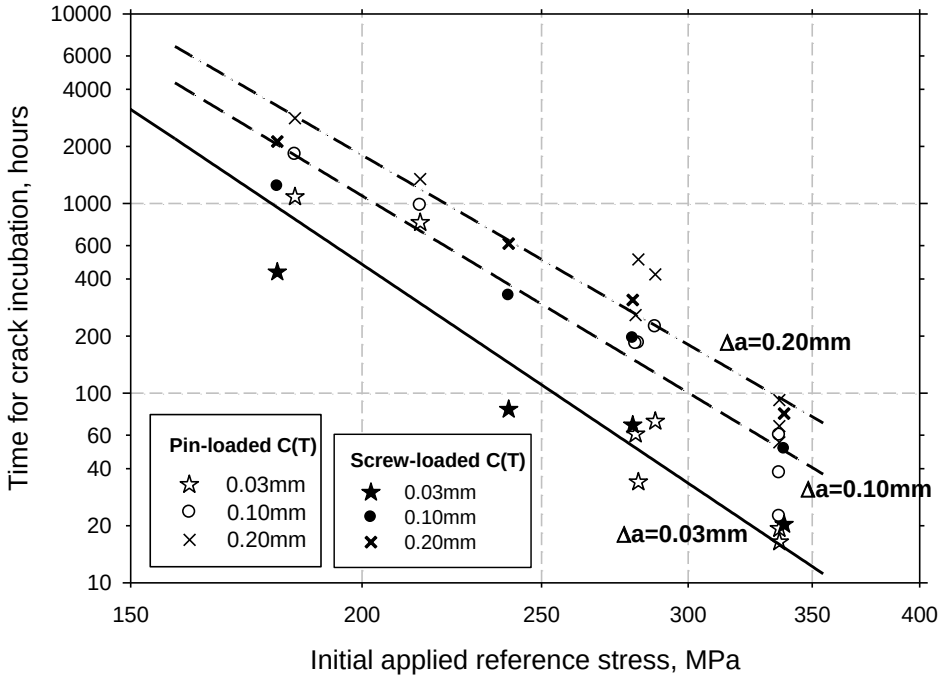

Figure 11 Times for crack incubation to various crack growth increments for Type 316H stainless steel C(T) specimens subjected to constant load at 550°C

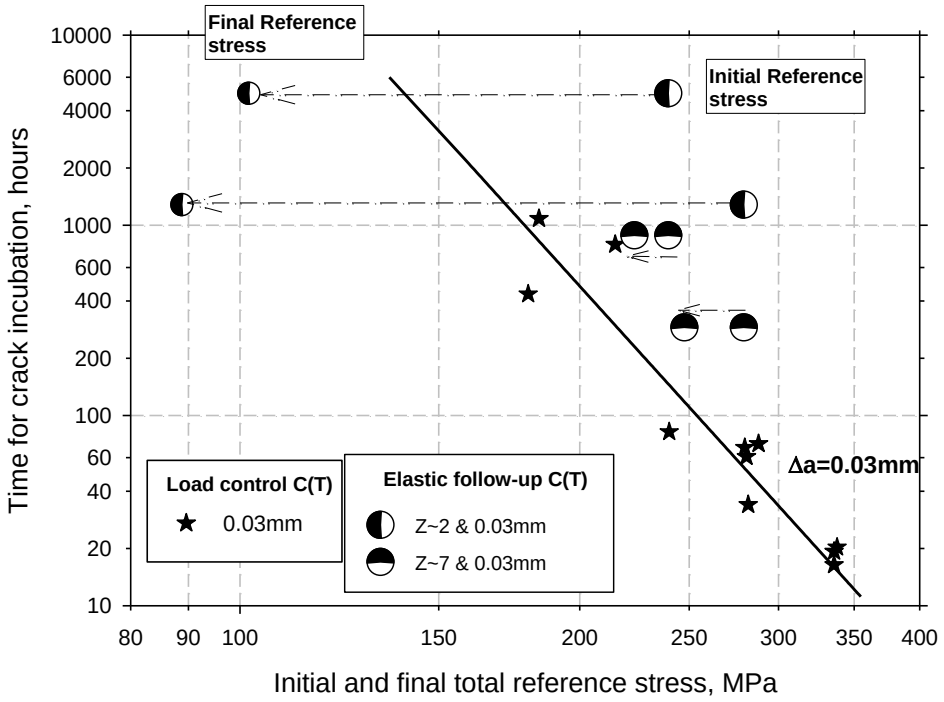

Figure 12 Times for crack incubation to a crack growth increment of 0.03mm for Type 316H stainless steel C(T) specimen for constant load and elastic follow-up conditions at 550°C. The elastic follow-up tests are shown with initial and relaxed total reference stresses.

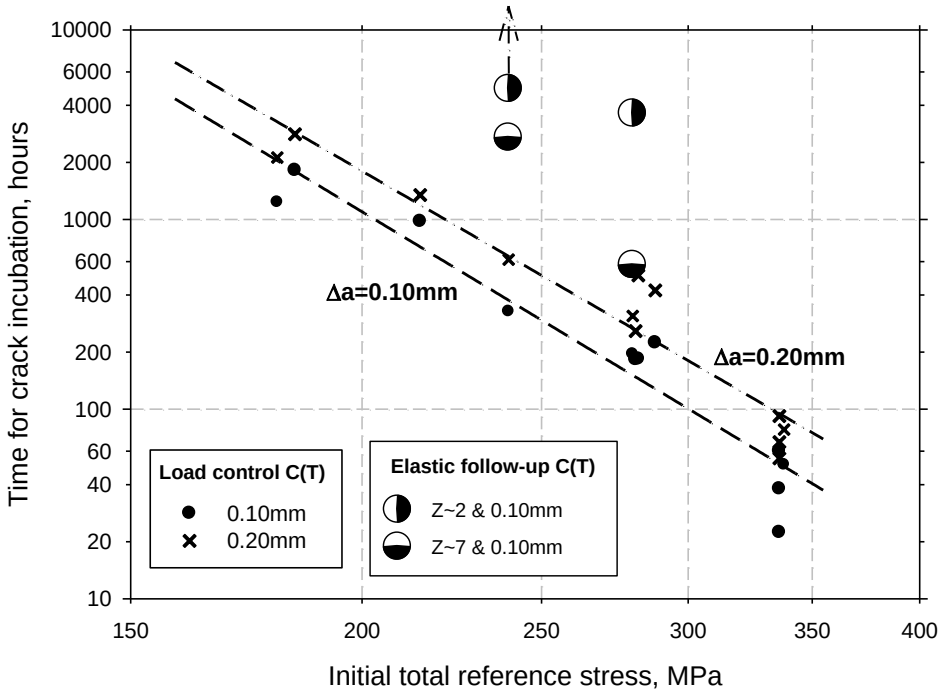

Figure 13 Times for crack incubation to various crack growth increments for Type 316H stainless steel C(T) specimen for constant load and elastic follow-up conditions at 550°C

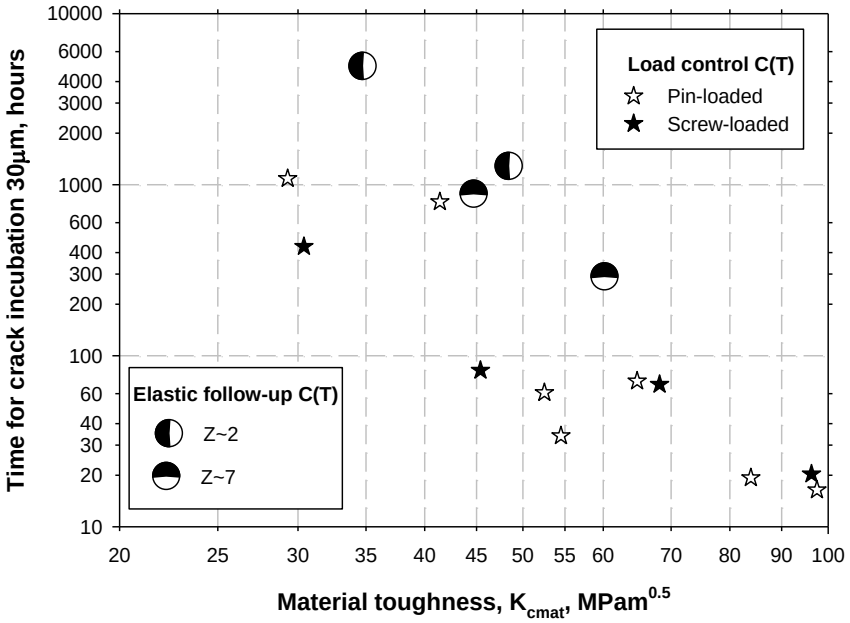

Fig 14 Times for crack incubation to 0.03mm for Type 316H stainless steel C(T) specimens under constant load and elastic follow-up conditions at 550°C